Optica Applicata, Vol. XXII, No. 2, 1992

On the problems of optimizing the reference sphere for interference measurements of wave aberrations as exemplified by the radial shearing

W. KOWALIK, B. DUBIK

Institute of Physics, Technical University of Wrocław, Wybrzeże Wyspiańskiego 27, 50–370 Wrocław, Poland.

During the measurements of wave aberrations of objectives some problems appear especially when high accuracy is required as is the case in interferometric methods. These problems are due to the fact that the real function describing the interference field is measured in a discrete form. It has been shown that the replacement of the continuous function by a discrete one as well as the way of data processing affect the accuracy of measurements. Some ways of improving the measurement accuracy are proposed.

1. Introduction

Let us assume that a bundle of rays emerges from an arbitrary point in the space and enters the pupil of the objective. If the object space is uniform, the wavefront entering the objective is perfectly spherical. After having passed through the optical system the bundle becomes convergent and focuses around certain point in the image space. This point is an image of the respective point in the object space which generates the due bundle of rays. An ideal aberration free optical system would focus the bundle in one point, while the wavefront at the exit pupil of the optical system would be a sphere. In contrast to this, an aberrated optical system focuses the bundle in certain region around the point rather than only at the point itself, which means that the wavefront in the exit pupil of the system has the form of certain surface different from sphere. The deviation from the sphere constitutes the wave aberration. Since in the measuring practice we do not knowing the said sphere as well as its position, we are forced to choose it by fitting it to the wavefront emerging from the optical system according to the suitable criterion, for instance, so that the rms of the aberration be the least possible.

In practice, the wavefront at the exit pupil of the optical system examined is measured by sampling it in many places in the pupil. Instead of the continuous function, we thus obtain a discrete function (defined only in certain points). This fact and the ways the respective interferograms are scanned as well as the methods of data processing affect the accuracy of the measurements. The present work is devoted to these problems and the final results contain the indications the fulfilment of which assures that the respective measurement problems will be solved with small measurement error.

The results presented concern the interference measurement of aberrations employing the so-called radial shearing. Earlier, we applied also the transversal shearing but the results were the same. The final conclusions concern all the kinds of interferometers used in wave aberration measurements.

The accuracy of wave aberration measurement depends on:

1. Measuring system (including the quality of its elements, especially that of shearing elements).
2. Measuring conditions.
3. Scanning system of interferograms (the setup and the method of preliminary computer processing of data).
4. Process of computer processing of data (method of processing until reaching the final results).

The first two types of errors described widely in the literature may be evaluated easily. From our measuring practice it follows that when the commonly known conditions for the setup (interferometer) and measurement process are fulfilled the errors mentioned in points 1 and 2 may be eliminated to such degree that the final error will be essentially affected only by errors 3 and 4. This article illustrates the possible magnitude of these errors while the emphasis is put on the errors of computer processing of the data and some errors introduced by the manner of scanning. Since this article is not devoted to the general methods of scanning, they will not be described (the corresponding literature is very rich). The problem discussed in this work concerns only the influence of the way both scanning and sampling are carried out on the computation errors of aberrations and the due averages necessary to calculate the optimal reference sphere. This is valid for all the methods of scanning including the modern ones exploiting the CCD TV camera, and FRAME GRABBERS and double Fourier transforms or discrete phase change.

2. Principle of determination of the wavefront by the method of radial shearing interferometry

To describe the wavefront in the exit pupil of an objective as well as the interferogram it is convenient to use the polar coordinate system (Fig. 1c). A real position of the site in the pupil is described by r', φ coordinates. Further, instead of r', we shall use also the normed coordinate $r = 2r'/d$, where d is a real diameter of the exit pupil of the examined objective.

The wavefront emerging from the objective is described by the function $g(r,\varphi)$; this wavefront constitutes simultaneously the input signal for the radial shearing interferometer. A characteristic feature of the shearing interferometer is that it generates two wavefronts g' and g'' connected mutually in certain rigorously defined way of the form

$$g'(r,\varphi) = K'\{g(r,\varphi)\}, \tag{1a}$$

$$g''(r,\varphi) = K''\{g(r,\varphi)\} \tag{1b}$$

where K' and K'' are afinite operators. K' is often an identity operator, and therefore

$$g'(r,\varphi) = g(r,\varphi). \tag{2a}$$

In the radial interferometer, K'' is the working operator, so that

$$g''(r,\varphi) = g(br,\varphi) \tag{2b}$$

where $b = d/d'$ is a real number (Fig. 1).

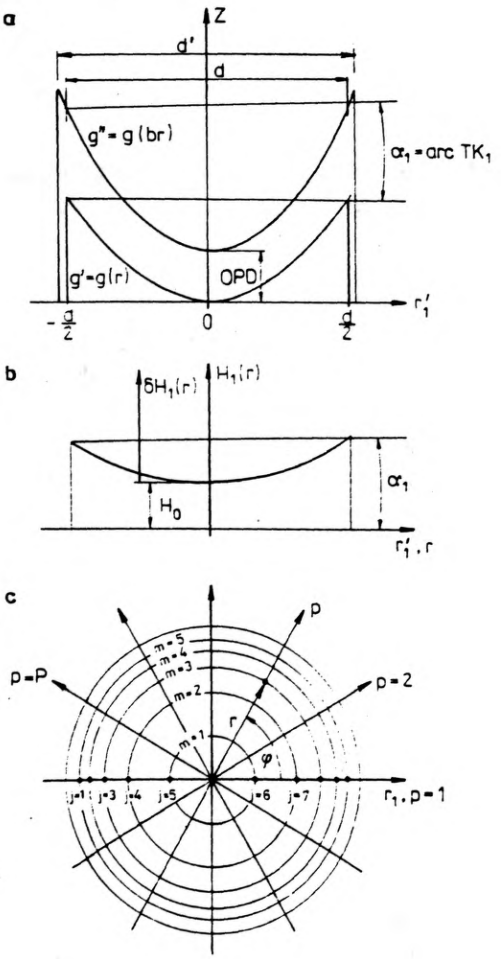

Fig. 1. Radial shearing interferometry. **a** — wavefronts, **b** — optical path difference, **c** — interferogram

Both the wavefronts generated in the radial shearing interferometer interfere with each other. The output signal of the interferometer is thus an area of interference, which is recorded in the form of an interferogram. The interference structure (for two-beam interference used in our experiments) is described by the equation

$$\text{INTENSITY } (r,\varphi) = 1+\cos\left[\frac{-2\pi}{\lambda} H(r,\varphi)\right] \tag{3}$$

where λ is a light wavelength for which the interference occurs, $H(r, \varphi)$ is an absolute difference of optical paths between the interfering wavefronts and is of the form

$$H(r, \varphi) = K''\{g(r, \varphi)\} - K'\{g(r, \varphi)\} + \mathrm{OPD} + \mathrm{TK}(\varphi) r \tag{4}$$

where OPD is the optical path difference introduced by the shearing element, which shears longitudinally the wavefronts, TK is the tilt between the interfering wavefronts. The relative optical paths difference, *i.e.*, the path difference defined with respect to a chosen reference point is described by the equation

$$\delta H(r, \varphi) = H(r, \varphi) - H_0 \tag{5a}$$

where H_0 is an absolute difference of optical paths of the reference point. From the dependences (1a), (1b), (2a), (2b), it follows that the relative optical path difference (measured with respect of the optical path difference of the reference point)

$$\delta H(r, \varphi) = g(br, \varphi) - g(r, \varphi) + \mathrm{TK}(\varphi) r + A \tag{5b}$$

may be defined with the accuracy up to a constant $A = \mathrm{OPD} - H_0$.

The above problem will be solved for the one-dimensional case, *i.e.*, for $\varphi = \mathrm{const}$. Hence, the information about the wavefront $g(r, \varphi)$ will be obtained separately along the subsequent scanning lines of this front. When choosing the reference point in the middle of the pupil of the objective examined and in the centre of the coordinate system at the intersection point of the scanning lines, the transition to a one-dimensional description becomes much simplified, owing to which Eq. (5b) will have the form

$$\delta H_\varphi(r) = g_\varphi(br) - g_\varphi(r) + \mathrm{TK}(\varphi) r + A. \tag{5c}$$

Let the sought wavefront $g_\varphi(r)$ be described by a polynomial of the form

$$g_\varphi(r) = \sum_{i=0}^{I} a_{i\varphi} r^i, \tag{6a}$$

hence,

$$g_\varphi(br) = \sum_{i=0}^{I} a_{i\varphi} b^i r^i \tag{6b}$$

where I is the order of this polynomial which results from the optimization of the dependence (7). The relative optical path difference between the interfering wavefronts may be described by optimal power polynomial

$$\partial H_\varphi(r) = \sum_{i=0}^{I} B_{i\varphi} r^i. \tag{7}$$

The order I of the polynomial is chosen separately for each polynomial according to criterion discussed in [1].

The following relations are valid for the coefficients $a_{i\varphi}$ describing the shape of the wavefront and the coefficients $B_{i\varphi}$ describing the relative optical path difference (which follows immediately from (5c) and (7) when taking account of (6))

$$a_{i\varphi} = \frac{B_{i\varphi}}{b^i - 1} \quad \text{for } i > 1,$$

$$a_{1\varphi} = \frac{B_{1\varphi} - \mathrm{TK}(\varphi)}{b-1},$$

$$a_{0\varphi} \; - \text{ undefined.} \tag{8}$$

As can be seen, the wavefront is known with the accuracy up to a constant (a_0 – undefined). The constant TK(φ) is unknown. The constant a_0 is not essential as far as the determination of wave aberrations is concerned, since the reference sphere is chosen for each given wavefront, and thus it is the problem of the reference system. The constant TK(φ) can be assumed to be equal to zero, if only the interference fringes on the interferogram are approximately centric with respect to the objective pupil. The inaccuracy of determination of $a_{1\varphi}$ resulting from such an assumption is corrected by the optimization of the reference sphere and does not affect the wave aberrations being determined. Thus, the knowledge of the parameter b (characterizing the interferometer) and the coefficients $B_{i\varphi}$ describing the relative path difference is sufficient to determine the shape of the wavefront. The determination of $g_{i\varphi}$ is reduced to the finding of $B_{i\varphi}$. For this purpose, the set of points $\{r_j, m_\varphi(r_j)\}$ is approximated by a power polynomial of the form (6a), where r_j is the j-th coordinate of the position of the interference fringe centre on a given scanning line (φ = const), and $m_\varphi(r_j)$ is the interference order corresponding to this coordinate. The relative optical path difference $\delta H(r) = \delta m(r)\lambda$, where $\delta m(r)$ is the relative difference of interference orders and λ – the light wavelength used. The relative order of interference $\delta m(r) = m(r) - m(r = 0)$ denotes the order of interference measured with respect to the reference point ($r = 0$).

3. Determination of the wave aberrations of objectives

The wavefronts of the real objectives are deformed as compared with the ideal spherical or plane wavefronts and thus they are aberrated. In order to examine the aberrations, a deviation of the real wavefront from the one being theoretically perfect must be determined.

Let a perfect wavefront – called here the reference sphere – be given by the function $S(r, \varphi)$. Thus, the wave aberration is described by a function defined as follows:

$$W(r, \varphi) = g(r, \varphi) - S(r, \varphi). \tag{9}$$

There are several ways of defining the reference sphere. In this work, a sphere fulfilling the criterion of minimum squared mean deviation from the given wavefront has been chosen

$$\iint [W(r, \varphi)]^2 \, dr \, d\varphi = \min. \tag{10}$$

The reference sphere defined in this way will be called optimal. In order to use

relation (10), the primary reference sphere must be preliminarily defined to enable calculation of the nonoptimal wave aberrations $W(r,\varphi)$. This sphere may be chosen quite arbitrarily. In [2] and [3], it was shown that the optimal aberrations for the continuous functions (calculated with respect to the optimal reference sphere) amount to

$$W'(r,\varphi) = W(r,\varphi) + Dr^2 + Kr\sin\varphi + Lr\cos\varphi + M. \tag{11}$$

The form of this relation has been given in the polar coordinates which are more suitable for the chosen way of scanning. The coefficients for relation (11) are [3]:

$$\begin{aligned} D &= -12\langle W(r,\varphi)r^2\rangle + 6\langle W(r,\varphi)\rangle, \\ K &= -4\langle W(r,\varphi)r\sin\varphi\rangle, \\ L &= -4\langle W(r,\varphi)r\cos\varphi\rangle, \\ M &= 6\langle W(r,\varphi)r^2\rangle - 4\langle W(r,\varphi)\rangle \end{aligned} \tag{12}$$

where the brackets denote the due averaging of the expressions over the whole area of the pupil

$$\langle W(r,\varphi)\rangle = \frac{1}{\pi}\int_0^{2\pi}\int_0^1 W(r,\varphi)\,dr\,d\varphi. \tag{13}$$

4. Practical realization

4.1. Measurement

The measurements have been made in monochromatic light of wavelength $\lambda = 0.6328$ μm generated by a He-Ne laser (Fig. 2). In order to expand the laser beam, a setup composed of a pinhole of 10 μm in diameter and a microscope

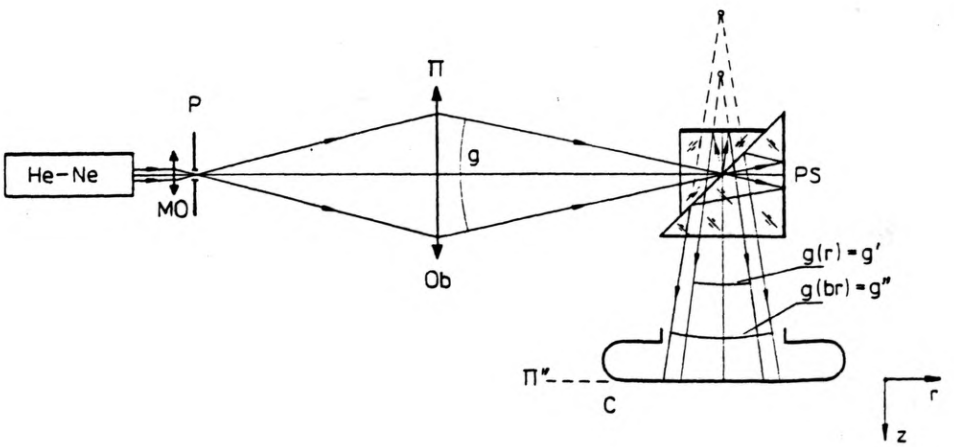

Fig. 2. Scheme of the radial shearing interferometer. He-Ne – helium-neon laser, MO – microscope objective, P – pinhole, Ob – tested objective, PS – shearing element, g – light beam examined, g', g'' – interfering light beams, Π'' – interferogram recording plane

objective was used. The examined beam g from the objective under test was divided into two beams with the help of a shearing element. The element PS is composed of two rectangular prisms ($40 \times 40 \times 40$ mm and $30 \times 30 \times 30$ mm) stuck to each other across one wall with an immersion fluid in between. The value of the optical path difference introduced by the element PS between the beams g' and g'' is changed by shifting one of the prisms with respect to another in the direction determined by the common plane of both prisms. The effect of interference of the separated beams g' and g'' was recorded in the plane Π'' (on the photographic emulsion). The result of a single experiment is recorded on the corresponding interferogram. Some examples of interferograms of the objectives examined are given in Figs. 3 and 4.

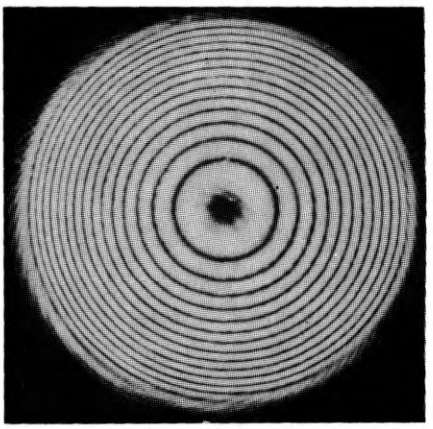

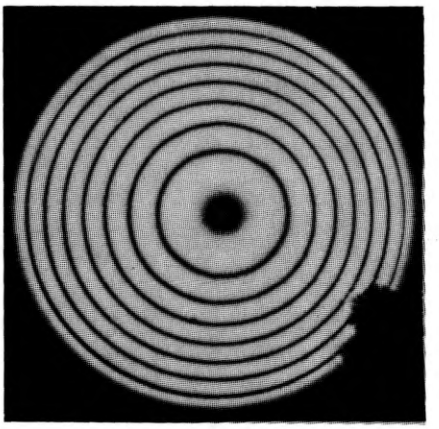

▲

Fig. 3. Interferogram of the telescope objective: $f = 500$ mm, $d = 50$ mm

Fig. 4. Interferogram of an uncorrected objective: $f = 155$ mm, $d = 47.9$ mm

4.2. Assumptions concerning the practical realization

i) As a primary reference sphere, such a sphere has been assumed which would overlap the wavefront surface at three points of coordinates $x = (-d/2,\ 0,\ d/2)$, with its centre laying in the (x, y) plane (Fig. 5).

ii) The radial scanning has been chosen because of the circular shape of fringes in the radial shearing. The scanning occurs along the scanning lines passing through the centre of the objective pupil (Fig. 1c). For all the scanning lines the centre of the pupil is a common pupil, which is salso the reference point (with respect to which the refractive orders of interference are measured). The description of the two-dimensional function may be then replaced by P one-dimensional functions.

iii) The digital data processing requires an introduction of discrete description of the functions. Thus, the functions are known only in sites. Therefore, the wave aberration in a site $W = W_{pq}$ will be understood as $W(r_{(q)}, \varphi(p)) = W(r, \varphi)$. The integration across pupil area (10) will be replaced by summing the due function values in sites of the scanning network. This will be possible when we presume that the assumption of equal density of the sites of the scanning networks, *i.e.*, the

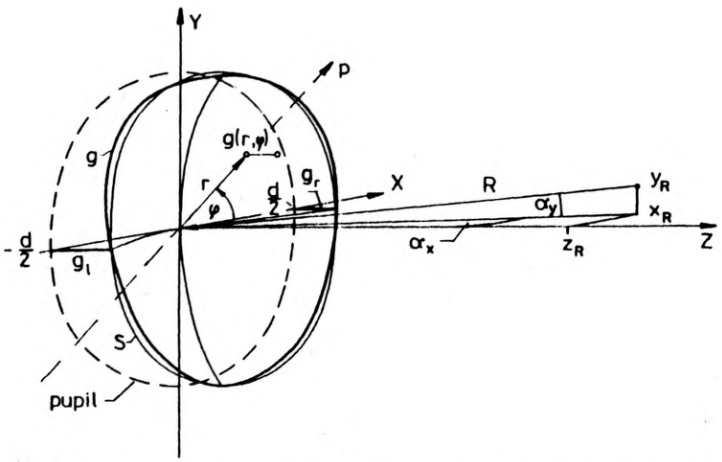

Fig. 5. Wavefront g and the reference sphere S in the exit pupil of the examined objective

number of sites over the unit area, is fulfilled across the whole pupil area. Relation (13) for N sites in the pupil takes the form

$$\langle W(r,\varphi)\rangle = \langle W\rangle = \frac{1}{N}\sum_{p}\sum_{q} W_{pq}. \tag{14}$$

It has been assumed that the sites of the scanning network are located only on the scanning line, which simplifies the mathematical procedures involved. In the accepted manner of scanning (Fig. 1c) there are $2Q+1$ sites ($q = 0, \pm 1, \ldots, \pm Q$). In the pupil, there are $N = 2PQ+1$ sites of the scanning network. In order to examine what the influence of the assumption of equal density on the result of measurement is two conditions have been adopted.

Condition 1 assumes that the normalized radius $r_{(q)}$ describes the position of the sampling point at the upper rim of the q-th zone which contains $2P$ sites on P scanning lines (Fig. 6a). Then (for $q = 1, \ldots, Q$) we have

$$r_{(q)} = \sqrt{\frac{2qP+1}{N}}. \tag{15}$$

Condition 2 assumes that the normalized radius $r_{(q)}$ describes the position of the sampling point located in the middle of the q-th zone (Fig. 6b). Then (for $q = 1, \ldots, Q$) we obtain

$$r_{(q)} = \sqrt{\frac{2qP-P+1}{N}}. \tag{16}$$

For both the cases an additional point (for $q = 0$) occurs in the centre of the pupil.

iv) From the assumption of the equal density, we derived the relations for the coefficients D, K, L, and M which differ from the coefficients for continuous function (12). For the discrete function, they have the forms:

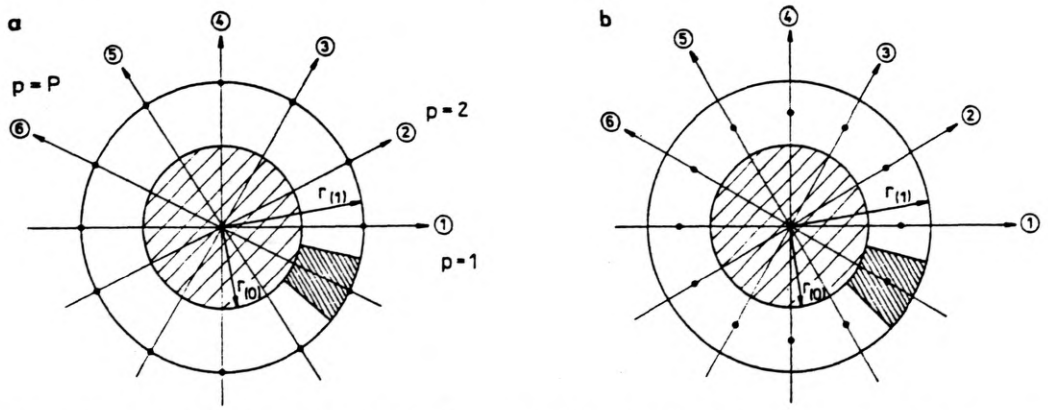

Fig. 6. Position of the sites with respect to the area attributed to one site (hatched region) according to **Condition 1** (15) – **a**, and according to **Condition 2** (16) – **b**

$$D = \frac{\langle W\rangle\langle r^2\rangle - \langle Wr^2\rangle}{\langle r^4\rangle - \langle r^2\rangle^2},$$

$$K = \frac{-\langle Wr\sin\varphi\rangle}{\langle (r\sin\varphi)^2\rangle},$$

$$L = \frac{-\langle Wr\cos\varphi\rangle}{\langle (r\cos\varphi)^2\rangle},$$

$$M = \frac{\langle Wr^2\rangle\langle r^2\rangle - \langle W\rangle\langle r^4\rangle}{\langle r^4\rangle - \langle r^2\rangle^2}. \tag{17}$$

v) The results presented in Section 5 are restricted to the case when there are $P = 6$ scanning lines and when the number of sites in the pupil takes three values: $N = 61$ $(Q = 5)$, $N = 121$ $(Q = 10)$, $N = 181$ $(Q = 15)$.

vi) The computer program SH allows us to calculate the wave aberrations for the radial and transversal shearing, respectively. We shall focus our attention on analysis of the results for radial shearing only, since the conclusions for transversal shearing are similar.

4.3. Analysis of an interferogram and the block scheme of the computer program for calculating the wave aberrations

Each of the interferograms is analysed along the radial scanning lines spaced by a constant angular value from one another. The basic information is gathered from the positions of the interference fringes and their interference orders, thus by the sets of data $\{r_j, m_\varphi(r_j)\}$, where r_j is a coordinate (in the radial coordinate system) of the dark (eventually bright) interference fringe on the p-th scanning lines and $m_\varphi(r_j)$ is the order of interference of the fringe of the coordinate r_j. For the chosen p-th scanning line $\varphi(p)$ [rad] $= (p-1)\pi/P$, when there are P scanning lines. The interferogram provides also information about the value of parameter b defining the magnitude of the wavefront g' with respect to the wavefront q''.

Introduction of data concerning position of interference fringes on P scanning lines $\{r_j, m_\varphi(r_j)\}$ where: $\varphi(p) = (p-1)\pi/P$, $p = 1, 2, \ldots, P$

↓

Approximation by the least square method involving orthogonal polynomial sets $\{r_j, m_\varphi(r_j)\}$, subsequently for all the scanning lines. The choice of optimal approximation I for each set separately. Results: functions $\delta H_\varphi(r)$ described by the coefficient sets $\{B_{i\varphi}\}$

↓

Calculation of the coefficients $\{a_{i\varphi}\}$ describing the wavefront $g_\varphi(r)$, for all the scanning lines

↓

Calculation of primary reference sphere passing through three points of the wavefront $g_\varphi(r)$ for $\varphi = 0$

↓

Calculation of primary wave aberrations W_{pq} at the sites of the scanning network

↓

Optimization of the reference sphere according to the criterion of the rms deviation from the wavefront. Coefficients D, K, L, M

↓

Calculation of the optimal wave aberrations W'_{pq} at the sites of the scanning network

Fig. 7. Block scheme of the SH program

On the basis of the above data, the shape of the wavefront $g_\varphi(r)$ for particular scanning lines can be determined, *i.e.*, the coefficient $a_{i\varphi}$ (4) can be found. A nonoptimal reference sphere passing through three points of the wavefront (on the scanning line $\varphi = 0$) has been fitted to the one-dimensional wavefront determined in the above way. Nonoptimal aberrations $W(r,\varphi)$ were calculated and next the reference sphere was optimized with respect to the criterion of minimum squared mean of aberration (across the whole exit pupil of the objective) and the optimal wave aberrations $W'(r,\varphi)$ for the examined objective were calculated. The block scheme of the program SH enabling the calculation of wave aberrations of the objective on the basis of data extracted from the radial shearing interferogram is presented in Fig. 7.

Since the program calculates the discrete values (*i.e.*, in the sites of the scanning network) the following magnitudes are also computed:

- arithmetic mean of the wavefront $\langle g \rangle = \Sigma g_{pq}/N$,
- rms $= \sqrt{\langle g^2 \rangle}$, where $\langle g^2 \rangle = \Sigma g_{pq}^2/N$,
- variance of the wavefront $= \sqrt{N(\langle g^2 \rangle - \langle g \rangle^2)/(N-1)}$, (18)
- arithmetic mean of the wave aberrations $WS = \langle W \rangle = \Sigma W_{pq}/N$,

– rms of aberrations $WS^2 = \sqrt{\langle W^2 \rangle}$, where $\langle W^2 \rangle = \Sigma W_{pq}^2/N$,

– variance of aberrations $= \sqrt{N(\langle W^2 \rangle - \langle W \rangle^2)/(N-1)}$.

The last three magnitudes are calculated for both nonoptimal and optimal aberrations. The nonoptimal reference sphere is calculated (in the sites) from the formula

$$S(r',\varphi) = R\left[1 - \sqrt{1 - \frac{(r'\cos\varphi - x_R)^2 + (r'\sin\varphi - y_R)^2}{R^2}}\right]. \tag{19}$$

The program enables calculation of magnitudes describing the reference sphere (Fig. 5). Thus for the nonoptimal sphere, the coordinates of the sphere centre and its radius are:

$$z_R = \frac{g_l^2 + g_r^2 + (d^2/2)}{2(g_l + g_r)}, \quad x_R = \frac{g_r^2 - g_l^2 + 2(g_l - g_r)z_R}{2d},$$

$$y_R = 0, \quad R = \sqrt{x_R^2 + y_R^2 + z_R^2}. \tag{20}$$

The magnitudes g_l and g_r are calculated during reconstruction of the wavefront from (6a), for a horizontal scanning line. For the optimal sphere we have:

$$R' = \frac{R}{1 - (8DR/d^2)}, \quad x'_R = R'\left(\frac{x_R}{R} + \frac{2L}{d}\right), \quad y'_R = R'\left(\frac{y_R}{R} + \frac{2K}{d}\right),$$

$$z'_R = z_R - R + R' - \frac{x_R'^2 + y_R'^2}{2R'} + \frac{x_R^2 + y_R^2}{2R} - M. \tag{21}$$

When deriving relations (21), we took advantage of (9) and of the formula

$$W'(r,\varphi) = g(r,\varphi) - S'(r,\varphi),$$

hence,

$$W'(r,\varphi) = W(r,\varphi) + S(r,\varphi) - S'(r,\varphi) \tag{22}$$

and from

$$S(r,\varphi) - S'(r,\varphi) = \frac{4Dr'^2}{d^2} + \frac{2Kr'\sin\varphi}{d} + \frac{2Lr'\cos\varphi}{d} + M. \tag{23}$$

5. Analysis of the results

The wave aberrations of the examined objectives were obtained as a result of the interferogram analysis and the calculations made with the help of SH program. In Figures 8 and 9, the wave aberration distributions in the pupils of the examined objectives are presented. In order to examine the influence of some solutions on the results, four versions of the same program have been elaborated, the names of which are specified below.

The comparison of the measurement results allows us to establish to what degree the final result of the aberration measurements is affected by the equal density

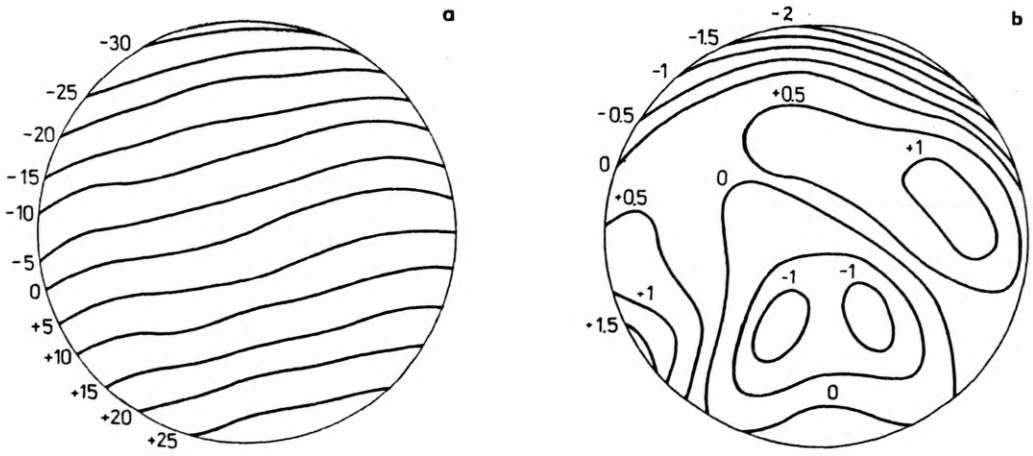

Fig. 8. Wave aberrations in λ units of the telescope objective $f = 500$ mm, $d = 50$ mm. **a** – nonoptimal. **b** – optimal. Parameters of the optimal reference sphere in λ units: $R' = 6252830.68$, $x'_R = -847.31$, $y'_R = 4554.56$, $z'_R = 6252829.25$

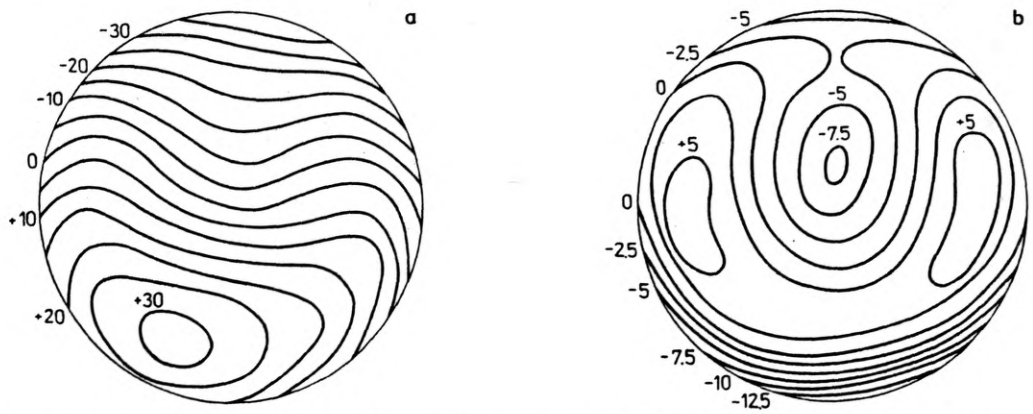

Fig. 9. Wave aberrations in λ units of the noncorrected objective $f = 155$ mm, $d = 47.9$ mm. **a** – nonoptimal, **b** – optimal. Parameters of the optimal reference sphere in λ units: $R' = 2781581.51$, $x'_R = 666.72$, $y'_R = 2418.31$, $z'_R = 2781586.66$

Condition for the radius of q-th zone. Site of q-th zone	Formulae for D, K, L, M for the functions	
	continuous (12) and (14)	discretized (17) and (18)
lies in the middle of the region of the surface attributed to 1 site (16)	SH 1	SH 2
lies at the rim of the region of the surface attributed to 1 site (15)	SH 3	SH 4

assumption for sites in the pupil or by the chosen relations for the coefficients D, K, L, M of the discretized function. The theoretical formulae for the discretized function

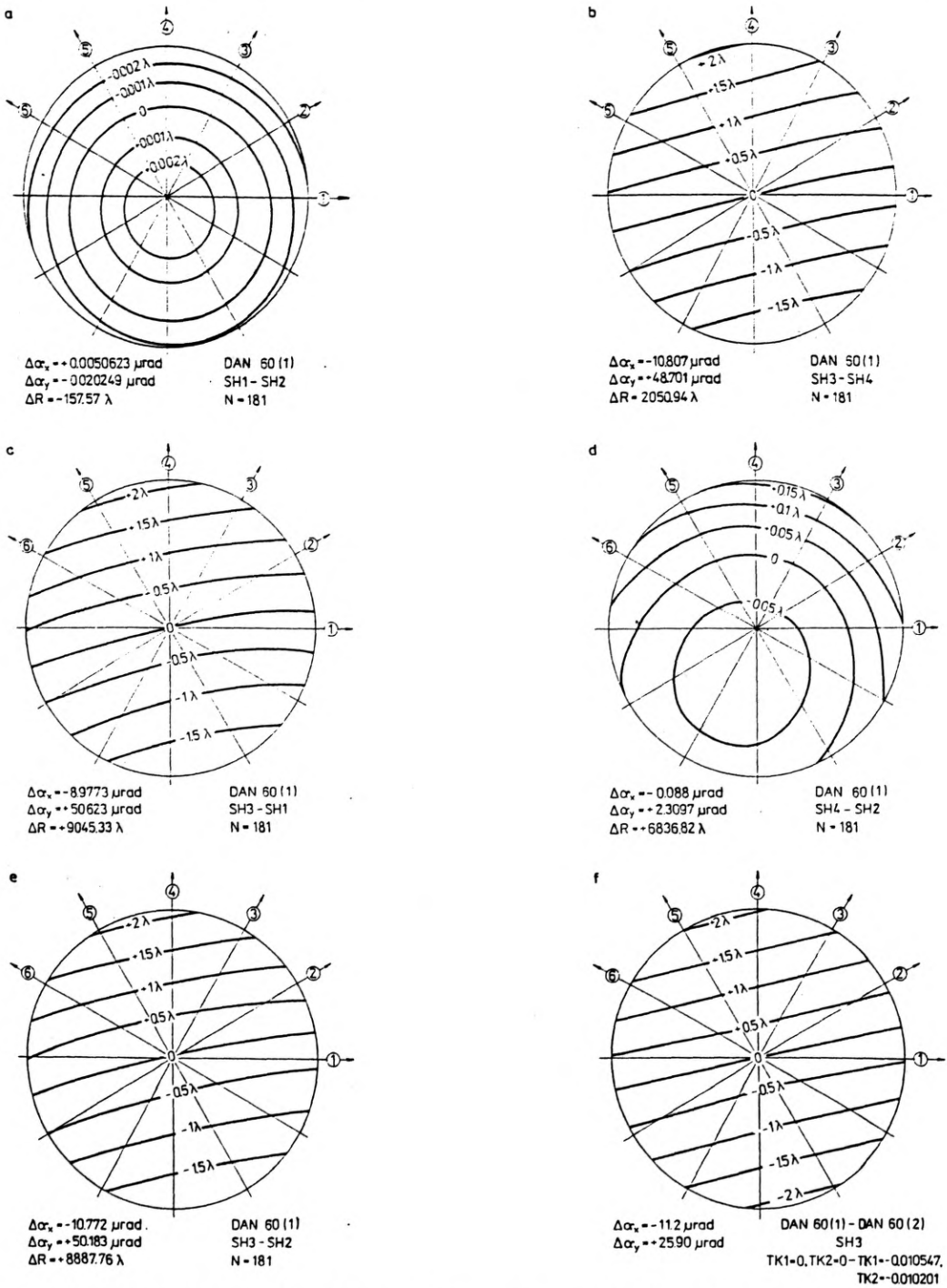

Fig. 10. Differences in wave aberrations or reference spheres obtained from the respective calculating programs. The results for the telescope objective. The operator Δ describes the differences in the tilt of spheres $\Delta\alpha$ or in the curvature radius of the sphere $\Delta R'$

for the coefficients D, K, L, M and the condition under which the site lies in the middle of the area (attributed to the site) fulfil better the due requirements concerning the accuracy of calculations. The program SH 2 should give the best results. In order to see it better, the differences in the results of optimal aberrations obtained by using the corresponding programs are shown in Fig. 10. These differences (with opposite signs) are at the same time the differences between the optimal spheres obtained using the corresponding programs.

Let us analyse Figure 10. When the site occurs in the middle of the area attributed to a single site, we obtain very small differences in the reference sphere (**a**, SH 1 – SH 2). When the site lies at the rim of the unity area these differences become very large (**b**, SH 3 – SH 4). A particularly great error concerns the slope of the spheres. If the formulae for the D, K, L, M coefficients for the continuous functions are used, the errors (**c**, SH 3 – SH 1) are of similar magnitude as those in Fig. 10**b**. Much smaller differences occur when using formulae for the D, K, L, M coefficients for discretized functions (**d**, SH 4 – SH 2). The greatest differences in the results occur when using the programs SH 3 and SH 2 (**e**, SH 3 – SH 2), when the conditions are fulfilled to the highest and lowest degree, respectively. Hence, it is clear that the program SH 2 is the best one, as could be expected. An additional proof is provided when testing the programs for different input data concerning the slope of the sphere (TK1 = TK2 = 0, TK1 and TK2 determined). The differences in the results occur only for the program SH 3 (**f**). The reason for this is that the assumption of equal density of sites in the pupil is not fully satisfied which becomes clear only when the formulae for the D, K, L, M coefficients for the continuous functions are concerned. This provides also the proof that the formulae for the said coefficients for discrete functions should be used. Not very rigorous fulfilment of the assumption of equal density of the sites in the pupil does not manifests itself in a very sharp way. Identical conclusions follow from Fig. 11 which illustrates the differences between the aberrations or spheres for a noncorrected objective. In Table 1, the general results of the measurements of the wave aberrations computed by four versions of the SH program for a telescope objective are presented.

T a b l e 1. Wave aberrations of a telescope objective [λ]. The averaged values from the whole pupil for $N = 181$

Aberrations	SH 1	SH 2	SH 3	SH 4
nonoptimal:				
arithmetic				
average WS	0.077196		0.107573	
rms WS^2	14.780990		15.301970	
optimal:				
arithmetic				
average WS	$0.113607 \cdot 10^{-4}$	$-0.756538 \cdot 10^{-10}$	−0.030468	$-0.832916 \cdot 10^{-10}$
rms WS^2	0.721097	0.721096	1.257464	0.752344

From the comparison of rms, it can be seen that the best selection of the reference spheres corresponds to the SH 2 program. The worst reference sphere has been chosen by using the SH 3 program. In Table 2, the results of average wave aberrations for the same objective obtained by using SH 1 and SH 2 programs for different number of sites in the pupil of the examined objective are presented. The reference sphere determined by these programmes is properly fitted.

T a b l e 2. Wave aberrations of a telescope objective [λ]. The averaged values from the whole pupil, for the different number of sites N

	SH 1	SH 2	N
Arithmetic average WS	$0.9494406 \cdot 10^{-4}$	$-0.135977 \cdot 10^{-10}$	61
	$0.2521531 \cdot 10^{-4}$	$-0.745635 \cdot 10^{-11}$	121
	$0.1136047 \cdot 10^{-4}$	$-0.756539 \cdot 10^{-10}$	181
rms WS^2	0.7161664	0.71611498	61
	0.7203413	0.72033784	121
	0.7210970	0.72109630	181

This can be seen better in Figure 12, where rms aberration for SH 1 and SH 2 (in this figure, a common continuous line due to small differences) is a nonlinear function increasing with the number of sites in the pupil. The increase of this function is obvious since the wavefront is rather complex and may be better recorded in the case of greater number of sites. The differences between the results obtained with the help of SH 1 and SH 2, respectively, are imaged by the broken line. As the number of points in the pupil increases, the results of both programs start to increasingly overlap. The differences in aberrations are less and less pronounced as the number of sites increases in the pupil. The program SH 2 in which the D, K, L, M coefficients are calculated for the discrete function tends quicker to their optimal values. Similarly, the differences (for the SH 1 and SH 2 programs) in both the positions of the optimal reference sphere centre ($\Delta x'_R$, $\Delta y'_R$, $\Delta z'_R$) and the value of the curvature radius $\Delta R'$ (Tab. 3) decrease linearly.

T a b l e 3. Differences in [λ] between the results describing the reference sphere obtained with the help of SH 1 and SH 2 programs

	$N = 61$	$N = 121$	$N = 181$
$\Delta R' = \Delta z'_R$	1345.34	350.71	157.57
$\Delta x'_R$	−0.457	−0.123	−0.071
$\Delta y'_R$	1.979	0.506	0.115

The program SH enables also the calculation of the aberrations depending only on the current radius in the pupil (Fig. 13). Then the averaging over index q, *i.e.*, over the angle φ in the pupil, is performed.

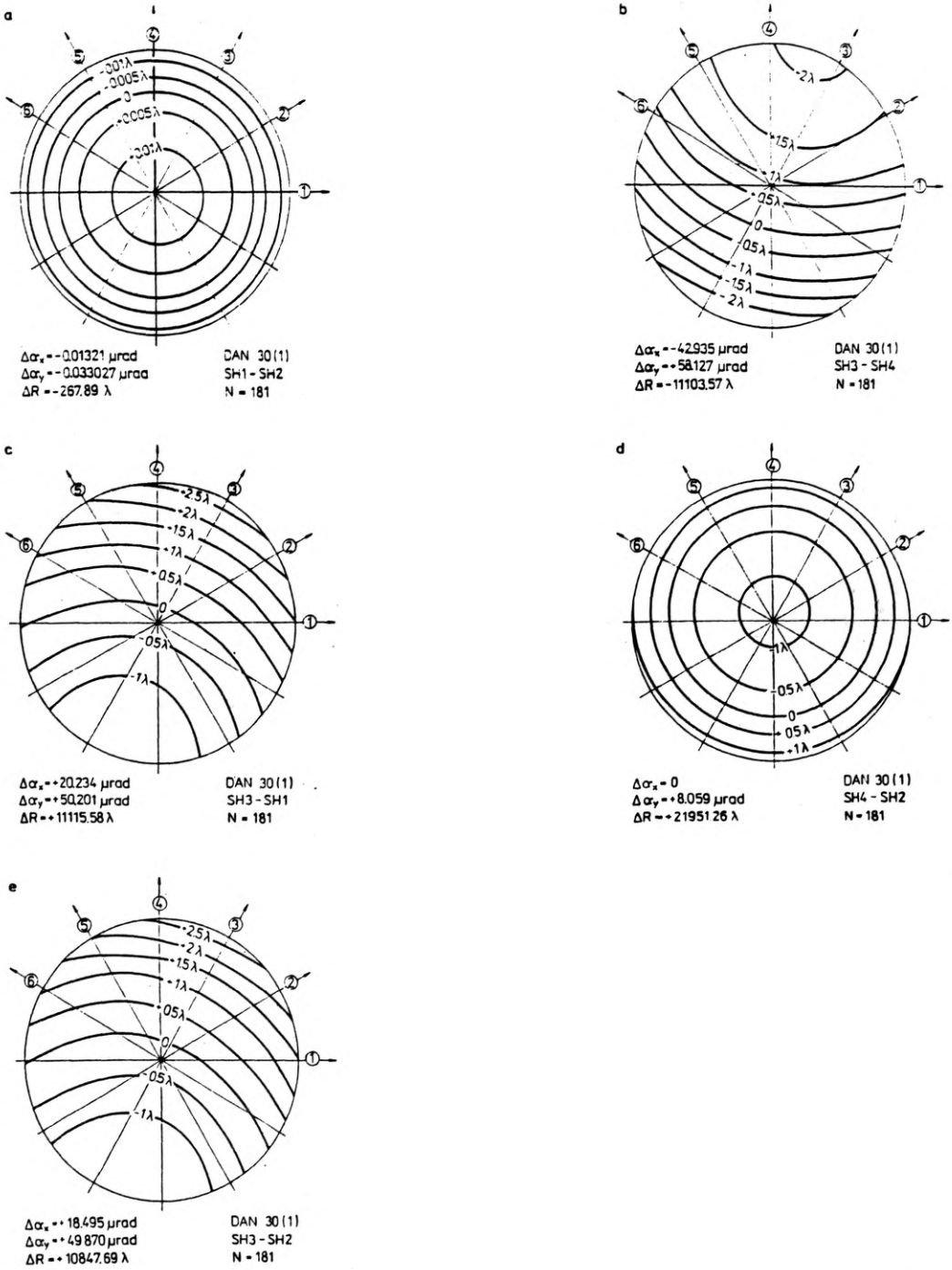

Fig. 11. Differences in wave aberrations or reference spheres obtained from the respective calculating programs. Results for the uncorrected objective The operator Δ describes the differences in the tilt of spheres $\Delta\alpha$ or in the curvature radius of the sphere $\Delta R'$

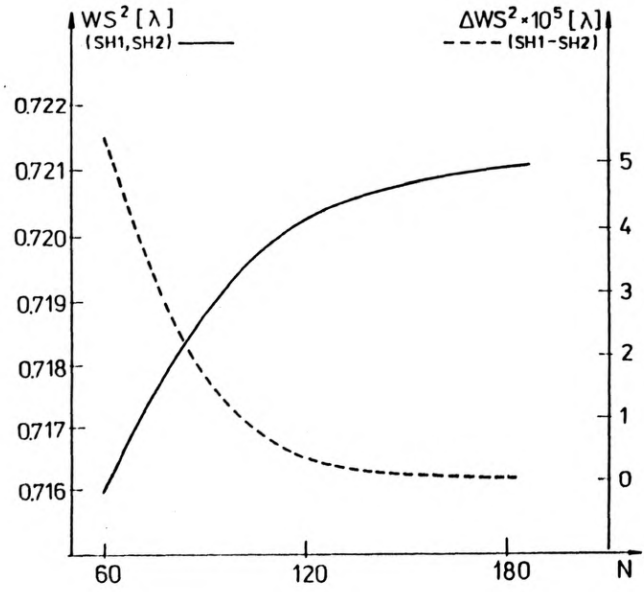

Fig. 12. Dependence of the squared average WS^2 of the aberration (continuous line) on the number of sites N in the pupil of the telescope objective. The results for the programs SH 1 and SH 2. Differences in squared average of the aberration ΔWS^2 obtained from programs SH 1 and SH 2

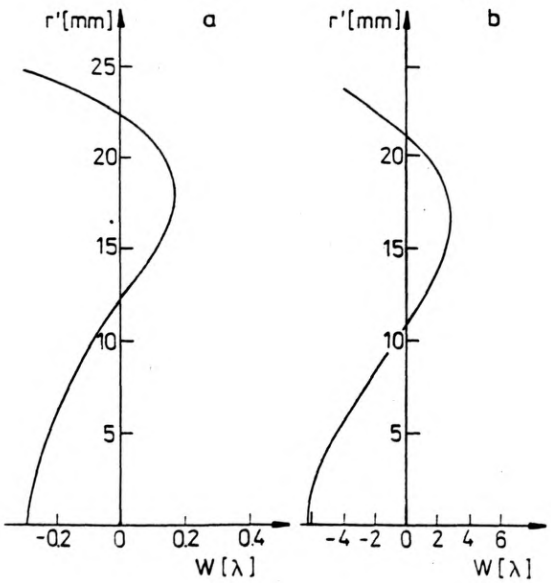

Fig. 13. Wave aberrations in the pupil averaged over the angle φ in the pupil for the telescope (a) and noncorrected (b) objectives. (As a noncorrected objective a cemented doublet being a part of a large objective was taken)

6. Remarks

During testing of the program the following remarks concerning the improvement of both accuracy and reliability of the calculating process may be taken into account:

1. The way of scanning assumed in this work facilitates considerably the data processing by computer. This is true both for the scanning system and the computer processing of data. We have shown that this method works very well so far as optimal fitting of the reference sphere (program SH 2) is concerned. We have applied it consciously, being interested in showing the simplest ways of solving. This method is not sufficient so far as the fidelity of aberration recovery is concerned. There are some regions in which the intersite distances are great as well as some where the said distances are very small. To obtain good fidelity another way of scanning is proposed (for instance, such as that in Fig. 14a or b).

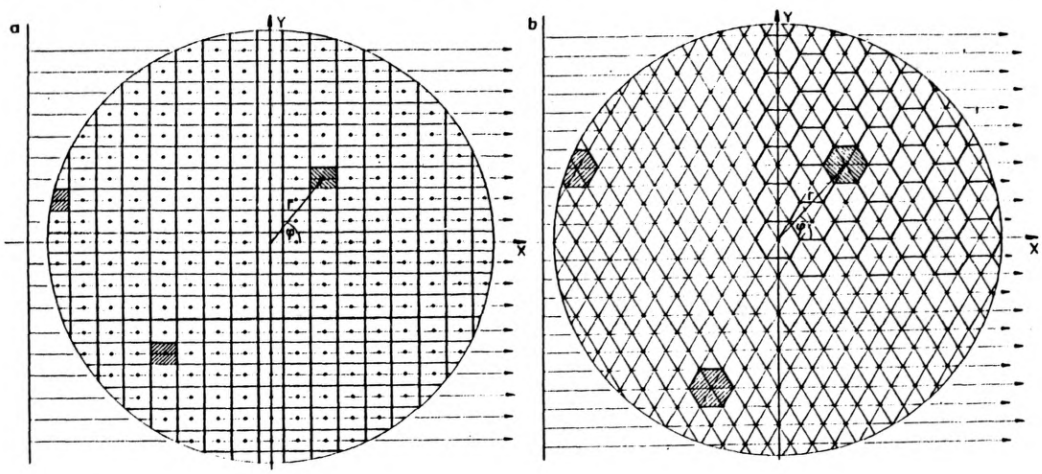

Fig. 14. Site network in the pupil and the areas (s_{pq} — hatched) corresponding to the sites. a — rectangular site network (scanning along the horizontal lines), b — triangular site network (hexagonal area of a site), scanning along the horizontal lines or along the lines in three different directions

In this case, the calculation of average values (14) should be replaced by weighted average values of the form

$$\langle W \rangle = \sum_p \sum_q \frac{s_{pq}}{s} W_{pq} \tag{24}$$

where s_{pq} is a surface attributed to a single site, while s is the surface of the examined objective. For the inside sites of the pupil the weight $s_{pq}/s = 1/N$ (since $s_{pq} = s/N$), while for the sites at the pupil rim (for which the area s_{pq} attributed to a single site is smaller, being restricted by the pupil diaphragm) the weight is s_{pq}/s (for $s_{pq} < s/N$). The calculations become slightly more complex but the fidelity of recovery is then very good while the assumption of constant density of sites in the pupil is fulfilled.

2. For very accurate measurement method and definite conditions of measurement another kind of error may appear. When deriving formulae (12) and (17) it has

been assumed that a paraboloid approximates very well the sphere. Therefore, the formula for the sphere has been replaced by the following expansion into series:

$$S(r') = z_R - R\sqrt{1-(r'/R)^2} = z_R - R + \frac{1}{2}\frac{r'^2}{R} + \frac{1}{8}\frac{r'^4}{R^3} + \frac{1}{16}\frac{r'^6}{R^5} + \ldots \tag{25}$$

in which only the first three components were taken into account. This assumption may cause the said error. In order to better approximate the sphere we take now account of the first four components. Then in place of (11), we obtain

$$W' = W + Dr^2 + Er^4 + Kr\sin\varphi + Lr\cos\varphi + M, \tag{26}$$

and, in place of (17), we obtain the relations of the form:

$$D = \frac{\langle W\rangle(\langle r^2\rangle\langle r^8\rangle - \langle r^4\rangle\langle r^6\rangle) + \langle Wr^2\rangle(\langle r^4\rangle^2 - \langle r^8\rangle) + \langle Wr^4\rangle(\langle r^6\rangle - \langle r^2\rangle\langle r^4\rangle)}{2\langle r^2\rangle\langle r^4\rangle\langle r^6\rangle - (\langle r^4\rangle^3 + \langle r^6\rangle^2) + \langle r^8\rangle(\langle r^4\rangle - \langle r^2\rangle^2)},$$

$$E = \frac{\langle W\rangle(\langle r^4\rangle^2 - \langle r^2\rangle\langle r^6\rangle) + \langle Wr^2\rangle(\langle r^6\rangle - \langle r^2\rangle\langle r^4\rangle) + \langle Wr^4\rangle(\langle r^2\rangle^2 - \langle r^4\rangle)}{2\langle r^2\rangle\langle r^4\rangle\langle r^6\rangle - (\langle r^4\rangle^3 + \langle r^6\rangle^2) + \langle r^8\rangle(\langle r^4\rangle - \langle r^2\rangle^2)}$$

$$K = \frac{-\langle Wr\sin\varphi\rangle}{\langle r^2\sin^2\varphi\rangle},$$

$$L = \frac{-\langle Wr\cos\varphi\rangle}{\langle r^2\cos^2\varphi\rangle},$$

$$M = \frac{\langle W\rangle(\langle r^6\rangle^2 - \langle r^4\rangle\langle r^8\rangle) + \langle Wr^2\rangle(\langle r^8\rangle\langle r^2\rangle - \langle r^4\rangle\langle r^6\rangle) + \langle Wr^4\rangle(\langle r^4\rangle^2 - \langle r^2\rangle\langle r^6\rangle)}{2\langle r^2\rangle\langle r^4\rangle\langle r^6\rangle - (\langle r^4\rangle^3 + \langle r^6\rangle^2) + \langle r^8\rangle(\langle r^4\rangle - \langle r^2\rangle^2)}. \tag{27}$$

Let us find out when either the formula (17) obtained by taking three first terms of the series or rather formula (27) obtained by accounting first four terms of series is suitable. For a telescope objective (Fig. 8) the application of formula (17) results in an error of the reference sphere on the rim of the pupil amounting to several $\lambda/100$. For the same objective, if the radius of the reference sphere were 10 times less this error would amount to 1λ, but when applying formula (27) it would be as small as 0.001λ. Generally, formula (27) may be applied under the following condition:

$$d[\text{mm}] > \delta m C, \quad \text{where } C = 128\lambda(R/d)^3 \tag{28}$$

where d, R and λ are expressed in mm, and δm represents the admissible limiting error for the sphere in $[\lambda]$ units and is given as a fraction of λ. The conditions for the measurement are determined by a ratio R/d. In Figure 15, the relation for the coefficient C is shown.

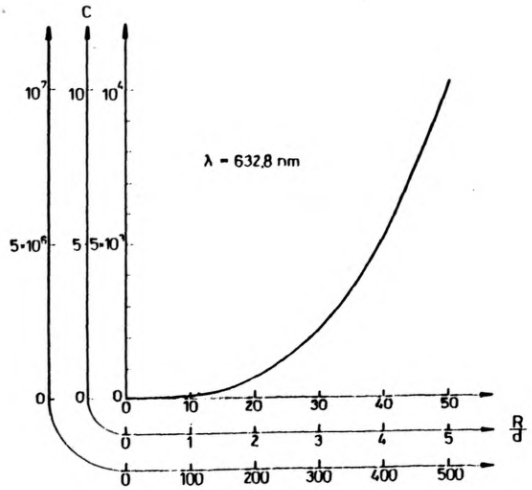

Fig. 15. Dependence of the C coefficient on the measurement conditions (R/d)

3. The primary reference sphere has been chosen on the basis of the wavefront values at three points on the horizontal scanning line. We have shown that the program SH2 takes account of all the tiltings of the sphere during its optimization very well. This, however, is based on very sharp assumption of equal density of sites in the pupil. Any inaccuracy in fulfilling this assumption may result in inaccurate compensation of the sphere tilting. In order to avoid such a situation it is more safe to base the choice of the primary reference sphere on two scanning lines: the horizontal X, and vertical Y, instead. The sphere may be chosen basing on three points (as previously) separately for each line. For the further calculations, we choose (according to (20)) R_x and x_R from the horizontal scanning line and R_y and y_R from the vertical scanning line. We calculate:

$$R = 1/2(R_x + R_y), \quad z_R = \sqrt{R^2 - (x_R^2 + y_R^2)}. \tag{29}$$

The primary sphere calculated in this way assures better stability of the final results than the primary sphere based on calculation taking one scanning line into account.

4. In order to assure a high fidelity a sufficient number N of sites of the scanning network must be chosen in the objective pupil.

5. Our program SH renders it possible to calculate the wave aberrations also for transversal shearing. All the relations given above are valid also for the last kind of interference. It should be only remembered that the more convenient form of scanning is then the choice of parallel scanning lines (parallel to the direction of the wavefronts shift) covering the pupil—interferogram. Also, in place of polar coordinates r, φ, it is more convenient to use the rectangular coordinates $\hat{x}$, $\hat{y}$ normed in the pupil. Then:

$$\hat{x} = r\cos\varphi, \quad \hat{y} = r\sin\varphi, \quad \hat{x}^2 + \hat{y}^2 = r^2. \tag{30}$$

6. In the case of radial shearing, an increase of absolute error in the middle of the

pupil of the objective under test is observed. It is a feature of this kind of interference which should be taken into account. This results from the small optical path differences existing in this region.

7. Conclusions

No additional analysis of measurement accuracy is made, since the examples considered seem to illustrate the program well enough and give the sources of the errors. Only general conclusions will be formulated and the corresponding way of treatment assuring high accuracy of the wave aberration measurement given.

1. How to choose a suitable way of scanning interferograms. In this respect there exist contradictory requirements. The scanning should assure a relative uniformity of measuring points (sites) in the pupil in order to enable a field approximation (in the simplest case the one-variable functions should be used). The scanning lines should be chosen taking account of the type of interference in order to assure high accuracy in the determination of the interference fringe middle position. The scanning lines should be possibly perpendicular to the fringes. For the transversal shearing it suffices that the scanning lines be parallel to the shearing shift. For the radial shearing the radial scanning is rather recommended. As a result of approximation the discrete values in the sites of the scanning network are obtained, while the distribution of sites should fulfil the assumption of constant density of sites in the pupil of the objective examined.

2. The primary reference sphere should be chosen on the basis of two mutually perpendicular scanning lines. It suffices to choose three data points on each of the lines.

3. The application of weighted averages is recommended. In particular, if the actual distribution of sites fulfils very well the assumption of steady density of sites the averages may be calculated without weight, but when calculating the averages, the sites at the pupil rim (see Fig. 14), the areas of which are cut by the pupil boundary, should be neglected.

4. The coefficients for the discrete functions may be calculated from either (17) or (27). For (27) when the number of sites is very large we recommended the calculation of average with the double precision in order to minimize the errors of computer processing of the data.

5. Optimal aberrations in the sites of the scanning network should be calculated.

6. If necessary, the following magnitudes may be calculated:

a) averages and squared averages of the optimal aberrations,

b) wave aberrations averaged over the angle φ,

c) parameters of the optimal reference sphere.

The procedures recommended above assure a high measurement accuracy.

In the measurement methods, employing CCD TV cameras and based either on double Fourier transform or on discrete phase change, a large number of samplings occurs which causes that the errors appearing in these methods are less than those presented above.

References

[1] DUBIK B., Opt. Appl. **10** (1980), 227; **11** (1981), 425; **12** (1982), 151.
[2] BORN M., WOLF E., *Principles of Optics*, Pergamon Press, Oxford 1964.
[3] PIETRASZKIEWICZ K., J. Opt. Soc. Am. **69** (1979), 1045.

Received December 22, 1991,
in revised form September 11, 1992